Autonomic Neuroscience: Basic and Clinical 228 (2020) 102699

Contents lists available at ScienceDirect

Autonomic Neuroscience: Basic and Clinical

journal homepage: www.elsevier.com/locate/autneu

The ectopy-triggering ganglionated plexuses in atrial fibrillation

Min-Young Kim[a,c,1], Belinda Sandler[a,c,1], Markus B. Sikkel[a,b,c], Christopher D. Cantwell[a,c], Kevin M. Leong[b,c], Vishal Luther[b,c], Louisa Malcolme-Lawes[b,c], Michael Koa-Wing[b,c], Fu Siong Ng[a,b,c], Norman Qureshi[b,c], Afzal Sohaib[b,c,d], Zachary I. Whinnett[b,c], Michael Fudge[b,c], Elaine Lim[b,c], Michelle Todd[b,c], Ian Wright[b,c], Nicholas S. Peters[a,b,c], Phang Boon Lim[a,b,c], Nicholas W.F. Linton[a,b,c], Prapa Kanagaratnam[a,b,c,*]

[a] Myocardial Function Section, NHLI, Imperial College London, UK
[b] Department of Cardiology, Imperial College Healthcare NHS Trust, London, UK
[c] Imperial Centre for Cardiac Engineering, Imperial College London, London, UK
[c] Barts Health NHS Trust, UK

ARTICLE INFO

Keywords:
Ganglionated plexus
Autonomic nervous system
Intrinsic cardiac nerves
Pulmonary vein ectopy
Atrial fibrillation

ABSTRACT

Background: Epicardial ganglionated plexuses (GP) have an important role in the pathogenesis of atrial fibrillation (AF). The relationship between anatomical, histological and functional effects of GP is not well known. We previously described atrioventricular (AV) dissociating GP (AVD-GP) locations. In this study, we hypothesised that ectopy triggering GP (ET-GP) are upstream triggers of atrial ectopy/AF and have different anatomical distribution to AVD-GP.

Objectives: We mapped and characterised ET-GP to understand their neural mechanism in AF and anatomical distribution in the left atrium (LA).

Methods: 26 patients with paroxysmal AF were recruited. All were paced in the LA with an ablation catheter. High frequency stimulation (HFS) was synchronised to each paced stimulus for delivery within the local atrial refractory period. HFS responses were tagged onto CARTO™ 3D LA geometry. All geometries were transformed onto one reference LA shell. A probability distribution atlas of ET-GP was created. This identified high/low ET-GP probability regions.

Results: 2302 sites were tested with HFS, identifying 579 (25%) ET-GP. 464 ET-GP were characterised, where 74 (16%) triggered ≥30s AF/AT. Median 97 (IQR 55) sites were tested, identifying 19 (20%) ET-GP per patient. > 30% of ET-GP were in the roof, mid-anterior wall, around all PV ostia except in the right inferior PV (RIPV) in the posterior wall.

Conclusion: ET-GP can be identified by endocardial stimulation and their anatomical distribution, in contrast to AVD-GP, would be more likely to be affected by wide antral circumferential ablation. This may contribute to AF ablation outcomes.

1. Introduction

Atrial fibrillation (AF) is most commonly caused by rapid electrical discharges from pulmonary veins (PV) (Haïssaguerre et al., 1998). Stimulation of the intrinsic cardiac autonomic nervous system, particularly the atrial ganglionated plexuses (GP) lead to shortening of PV and atrial refractory periods, causing AF (Schauerte et al., 2001). GP are large and dense clusters of nerves in the epicardium of the heart, particularly in the atria (Armour et al., 1997). Clinical studies have used high frequency stimulation (HFS) to functionally identify GP in the endocardium. Commonly, HFS is delivered continuously over several seconds to observe for atrioventricular (AV) dissociation or block, causing significant RR prolongation compared to baseline (Scanavacca et al., 2006; Patterson et al., 2005). We previously mapped the AV dissociating GP (AVD-GP) in the left atrium (LA) of patients with AF, and found that they did not correlate to all topographically studied GP locations (Armour et al., 1997; Kim et al., 2018). AVD-GP were commonly targeted by previous GP ablation studies, which produced mixed results (Scanavacca et al., 2006; Pokushalov et al., 2009; Driessen et al., 2016).

* Corresponding author at: Cardiology Department, St Mary's Hospital, Praed Street, W2 1NY, UK.
E-mail address: p.kanagaratnam@imperial.ac.uk (P. Kanagaratnam).
[1] Joint first authors for equal contribution to the study

https://doi.org/10.1016/j.autneu.2020.102699
Received 28 December 2019; Received in revised form 27 June 2020; Accepted 9 July 2020

Another method for identifying autonomic sites is to deliver bursts of HFS within the local atrial refractory period (synchronised to paced stimuli; "synchronised HFS"), avoiding direct high-rate myocardial capture like in continuous HFS. Synchronised HFS can reproducibly trigger atrial ectopy and/or AF/AT from sites distant to stimulation (Schauerte et al., 2001; Lim et al., 2011a). We termed these GP as "ectopy triggering GP" (ET-GP) and we noted that these sites did not always produce an AV dissociating effect. However, the initiation of ectopy and AF made these sites appealing targets as upstream triggers for AF. In order to further understand the role of ET-GP in the mechanism in AF, we tested the hypothesis that ET-GP have a different distribution pattern to that which we have previously described.

2. Methods

Patients with symptomatic, paroxysmal AF undergoing first ablation procedure were recruited to the study. We selected patients between 18 and 85 yrs. old, who were suffering from paroxysmal atrial fibrillation, had failed medical therapy and had been referred for ablation therapy. Anyone taking amiodarone was off it for at least 60 days, and off other antiarrhythmics and betablockers for five half-lives before the procedures. The full inclusion and exclusion criteria are in Table 1. Patients gave written informed consent and the study had ethics approval from the Health Research Authority and the Local Research Ethics Committee.

All patients had general anaesthesia and transthoracic oesophageal echocardiogram (TOE) to rule out left atrial appendage thrombus at the start of their procedures. Transseptal punctures were guided by TOE and fluoroscopy to access the left atrium. The CARTO™ system was used (Biosense Webster, Inc.) for 3D electroanatomical mapping of the left atrium. A decapolar catheter was positioned in the coronary sinus. A 20-pole circumferential catheter (LassoNav, Biosense Webster, Diamond Bar, CA, USA) was used to create a respiratory-gated 3-dimensional electroanatomic map of the LA (CARTO™, Biosense Webster, CA, USA). It was then positioned in the nearest PV to where HFS was being tested in the LA (e.g. left superior PV if HFS tested in the left side of the anterior wall, or left roof). A bipolar 3.5 mm irrigated-tip contact force sensing ablation catheter (Smart-Touch™, Biosense Webster, CA, USA) was used for pacing and delivering HFS. Blood pressure was continuously monitored using a radial arterial line. Heparin was administered throughout the cases to maintain the activated clotting time > 300 s.

2.1. Mapping for ET-GP using synchronised HFS

An S88 Grass stimulator (Astro-Med, RI, USA) was used to perform synchronised HFS to map for ET-GP. First, the ablation catheter was positioned at a stable site in the left atrium, aiming > 3 g of tissue contact. Also, the left side of the atrium was mapped first, as we often found more ET-GP in these regions. Secondly, the left atrium was paced at a higher rate than the intrinsic rate, using the ablation catheter with high output (10 V) at the distal poles. This checked for consistent atrial capture, no spontaneous atrial ectopy or ventricular capture. Ventricular capture was avoided with high output pacing first, in order to avoid capturing the ventricle with HFS which may cause ventricular arrhythmias. HFS was then synchronised to each pacing stimuli with 80 ms train duration, for up to 15 trains if no ectopy or AF. If atrial ectopy or AF occurred, pacing and HFS were stopped immediately. The same site was re-tested for reproducibility if synchronised HFS triggered ≤3 ectopy. A reproducible atrial ectopy and/or AF/AT triggering response to synchronised HFS was defined as "ET-GP". If there was no response to HFS, it was deemed a "negative HFS" site. Both ET-GP and negative HFS sites were tagged on the CARTO™ 3D left atrial geometry. If AF was sustained for more than 2 min, direct DC cardioversion was performed up to three times to revert the patient back into sinus rhythm and continue with the synchronised HFS protocol. The LA was globally mapped with HFS, aiming to test at least 80 HFS sites evenly distributed around the LA. Each HFS tested points were within 6 mm distance from each other. HFS was avoided in the left atrial appendage, mitral annulus where there was ventricular capture with pacing, and within the pulmonary veins. All data were recorded at 1000 Hz by the EP recording system (Bard EP, Lowell, MA, USA).

2.2. Ablation protocol

All patients underwent ET-GP ablation with or without pulmonary vein isolation after completing HFS mapping in the LA. These patients underwent 12-month follow-up with multiple Holter monitors as part of another pilot study to assess safety and feasibility of ET-GP ablation. We have not reported the outcomes of the ablation in this paper, as the ablation strategy was heterogenous and the numbers are too small to draw any conclusions on the clinical effect.

2.3. The probability distribution atlas of ET-GP

At the end of procedures, the LA fast anatomical maps of all patients

Table 1
Inclusion and exclusion criteria of the study.

Inclusion criteria	Exclusion criteria
• Males or females from 18 to 85 yrs. old • Paroxysmal atrial fibrillation • Off amiodarone for at least 60 days • Suitable candidate for catheter ablation • No previous left atrial ablation • Signed informed consent	• Contraindication to catheter ablation • Contraindication for general anaesthetic • Presence of cardiac thrombus • Previous left atrial ablation • Valvular disease that is grade moderate or greater • Any form of cardiomyopathy • Severe cerebrovascular disease • Active gastrointestinal bleeding • Serum Creatinine > 200umol/L or on dialysis or at risk of requiring dialysis • Active infection or fever • Life expectancy shorter than the duration of the trial • Allergy to contrast • Moderate to severe heart failure and/or NYHA Class III-IV • Bleeding or clotting disorders or inability to receive heparin • Uncontrolled diabetes (HbA1c ≥73 mmol/mol or HbA1c ≤64 mmol/mol and Fasting Blood Glucose ≥9.2 mmol/L) • Malignancy needing therapy • Pregnancy or women of childbearing potential not using a highly effective method of contraception • Unable to give informed consent or has insufficient comprehension

(NYHA = New York Heart Association).

were exported from CARTO™. A representative LA anatomy was chosen as a reference shell and all exported maps were co-registered onto this geometry using a semi-automated process (Ali et al., 2015). Further technical details of this process are described in our AVD-GP mapping study (Kim et al., 2018). A probability of 1 was applied to ET-GP sites and 0 for negative HFS response sites. Only HFS tested sites were included. Each measurement site was weighted by a Gaussian kernel with a variance of 5 mm, which characterised the uncertainty in the measurement of the site location as a result of catheter movement. The probability that an arbitrary test point within the reference atrial surface that has an ET-GP response was then computed per-patient. This was the sum of the product of probabilities of nearby measured sites with their respective weight kernels evaluated at the required point which was then normalised by the sum of the weight kernels evaluated at the point. Resulting maps were then averaged across the patients.

2.4. Statistics

Continuous variables that followed a normal distribution with small measure of spread were expressed as mean and standard deviation (mean ± SD). Continuous variables with skewed distribution and larger measure of spread were expressed as median and interquartile range (IQR).

3. Results

26 patients were recruited. Table 2 shows patient demographics and clinical characteristics. A range of reproducible responses were observed with synchronised HFS, characterised as follows.

3.1. AV dissociation with synchronised HFS

AV dissociation is the hallmark GP stimulation effect observed with continuous HFS but is also seen occasionally during synchronised HFS. Fig. 1A shows progressive Wenckebach until asystole. Re-testing the same site with continuous HFS produced a more pronounced AV dissociation, confirming the site as AV dissociating GP (AVD-GP). Less frequently, Wenckebach was followed by atrial ectopy and AF with synchronised HFS (Fig. 1B and C), identifying both AVD-GP and ET-GP at a single test site.

3.2. Atrial ectopy and arrhythmia with synchronised HFS

A PV ectopy triggered by synchronised HFS at an ET-GP site was mapped and visualised using CARTOFINDER®. Fig. 1D and Supplementary Video 1 show a step-by-step PV ectopy activation sequence and suggests that atrial ectopy induced by HFS is not the result of direct myocardial capture, but a distant neural effect that occurs remotely to the stimulation site.

Further example of PV ectopy triggered by synchronised HFS is shown in Fig. 2. Similar PV activation sequence is seen in Fig. 2A, B and C after stimulating three different HFS sites in the LA. However, Fig. 2A HFS triggers single PV ectopy only, whereas Fig. 2B and C trigger short run of AF and sustained AF respectively. The mechanism for these varied responses is yet to be determined but illustrates how the neural network can act on a single PV from multiple sites. Also, fewer HFS trains were needed for a more profound myocardial response each time at the same PV end-location. Similar phenomenon was also seen by stimulating the same HFS site and the examples are in the reproducibility section. The range of responses to ET-GP stimulation was seen in most patients and the distribution of this range in a single patient is shown in Supplementary Fig. 1.

We analysed and categorised 464 HFS sites into: < 3 beats of atrial ectopy (187 sites, 40%), < 30s of atrial arrhythmia (203 sites, 44%), > 30s of atrial arrhythmia (74 sites, 16%).

Table 2
Demographics of patients recruited to the study.

Demographic characteristics	
Age (yrs)	60 ± 9
Sex (male)	18 (69.2%)
Body mass index (kg/m^2)	27.7 ± 5.3
Left ventricular Ejection fraction (%)	64.5 ± 1.2
Left atrial diameter (cm)	3.69 ± 0.41
CHA_2DS_2-VASc	1.2 ± 0.9
0	8 (30.8%)
1	9 (34.6%)
≥2	9 (34.6%)
Stroke/ Transient ischaemic attack	1 (3.8%)
Coronary artery disease	1 (3.8%)
Hypertension	6 (23.1%)
Diabetes mellitus	1 (3.8%)

Continuous variables represented as mean ± SD. Categorical variables represented as numbers (%).

3.3. Reproducibility of atrial ectopy from ET-GP stimulation

Spontaneous ectopy occurs during AF mapping procedures. Therefore, it is important to prove that the observations described in Figs. 1 and 2 are reproducible and are driven by neural stimulation via synchronised HFS, rather than as spontaneous events. All synchronised HFS sites provoking single and short run of ectopy were re-tested from the same location at least twice for reproducibility (Fig. 3A). Sometimes, this triggered non-sustained AF (Fig. 3B). This type of potentiation confirms the reproducibility of neural stimulation even though the effect is more pronounced. Fig. 3C demonstrates an example from a different patient where the same location triggers an almost identical ectopy followed by non-sustained AF on both occasions. These observations confirm that ET-GP sites are anatomically fixed. In total, 150 ET-GP sites were tested at least twice in 26 patients. 118 (79%) retested positive, and 32 (21%) retested negative.

Similarly, negative HFS sites were also reproducible and anatomically fixed (Fig. 3D). We tested a negative site five times and no ectopic responses were elicited. This was repeated in 10 patients to prove that negative sites remain negative.

3.4. Quantification of ET-GP in the LA

A total of 2302 sites were tested with synchronised HFS in the LA, which identified 579 (25%) ET-GP. A median of 97 (IQR 55) HFS sites were tested per patient, which identified a median of 19 (20%; IQR 12) ET-GP per patient. The number of ET-GP ranged widely from one patient to another (Supplementary Fig. 2). There was no direct relationship between the number of HFS tested and the number of ET-GP identified (Supplementary Fig. 3).

3.5. The probability distribution atlas of ET-GP

Registration of all our patients to one reference shell revealed that 58.3% of the total surface area of the LA contained 90% of ET-GP. The average target registration error was 2.78 ± 1.05 mm (where '0' is perfect registration). The probability atlas of ET-GP across the whole LA revealed 30–40% probability of ET-GP in the following anatomical regions: the roof, around the ostia of all PVs except for the base of the right inferior PV in the posterior wall, mid anterior wall, left side of the anterior wall near the right superior PV and left side of the posterior wall near the left inferior PV. Smaller, discrete patches of ≥40% probability of ET-GP was confined to the PV region: left sided PV carina, right superior PV antrum and its ostium in the roof (Fig. 4).

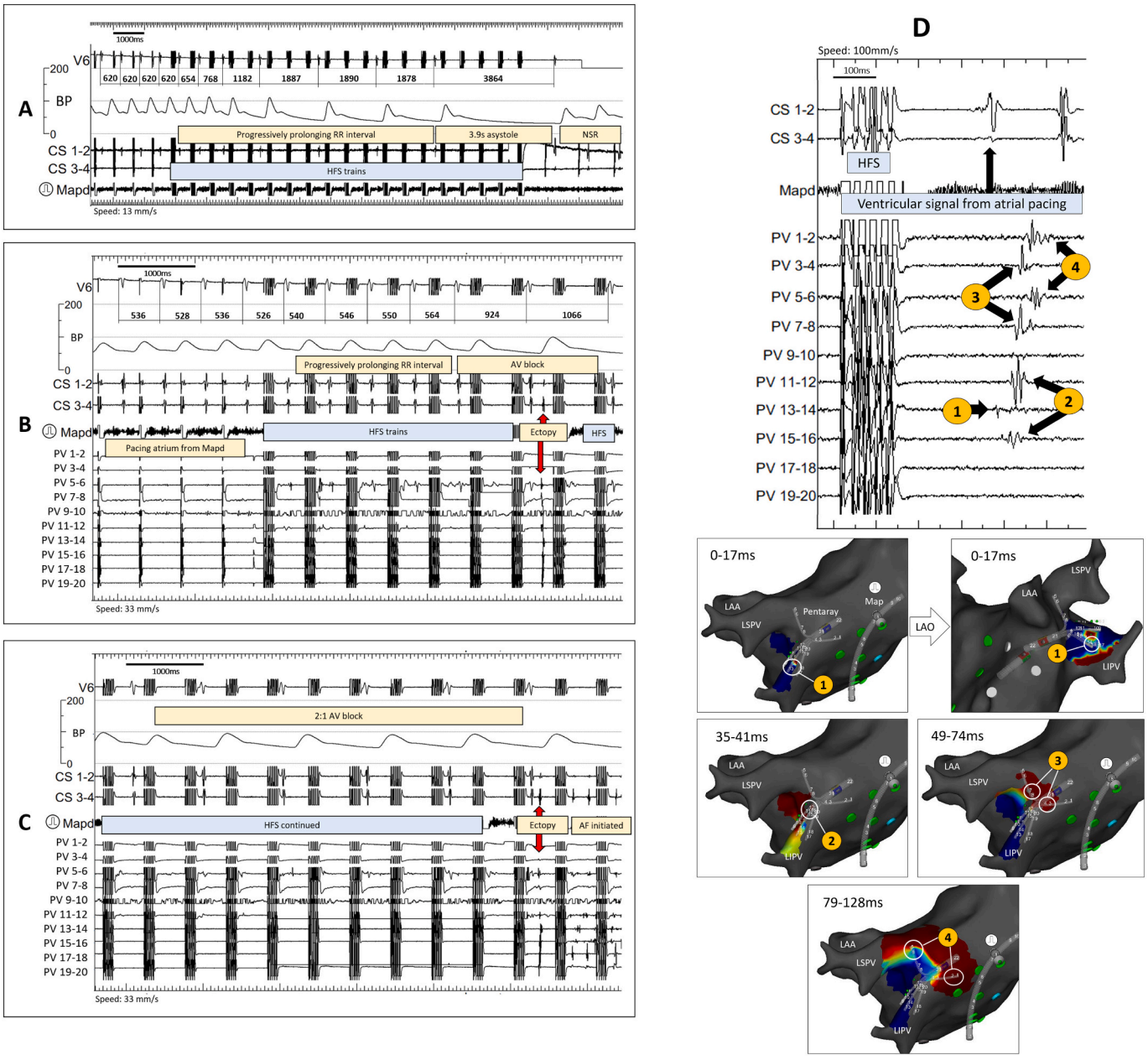

Fig. 1. Intracardiac electrograms of synchronised HFS at a GP site. Pacing and HFS were delivered from Map distal.
A) Pacing before the onset of HFS did not cause Wenckebach (620 ms). HFS was delivered after the fourth paced beat. There was a progressive RR prolongation during HFS until 3.9 sec asystole. RR interval recovered after cessation of HFS. No atrial ectopy or arrhythmia was observed. Therefore, this site was tagged as "AVD-GP".
B) Pacing before the onset of HFS did not cause Wenckebach (528-536 ms). There was a progressive RR prolongation during HFS until it reached 1066 ms; almost twice as long as the RR interval before HFS. An atrial ectopy was triggered after the 7th train of HFS. Therefore, this site was tagged both as "ET-GP" and "AVD-GP".
C) Continuation from the trace in B). AV block continued in 2:1 block fashion after the initial ectopy in B). Another ectopy was triggered after the 20th train of HFS, which induced AF. However, this second ectopy and AF induction may have been secondary to HFS capturing the myocardium due to shortening of the atrial refractory period following the initial atrial ectopy triggered in Fig. 1C.
(AV = atrioventricular, AVD-GP = atrioventricular dissociating ganglionated plexus, CS = coronary sinus, ET-GP = ectopy triggering ganglionated plexus, GP = ganglionated plexus, HFS = high frequency stimulation, LAA = left atrial appendage, LAO = left anterior oblique, LSPV = left superior pulmonary vein, LIPV = left inferior pulmonary vein, Map = mapping catheter, PV = pulmonary vein). (For interpretation of the references to colour in this figure legend, the reader is referred to the web version of this article.)

3.6. Comparison of ET-GP and AVD-GP probability distribution

A comparison was made between the ET-GP and the AVD-GP probability distribution atlases (Kim et al., 2018). A clear contrast was seen in the anatomical distribution of the two GP subtypes. This was particularly apparent in the roof, floor and the posterior wall of the LA. This illustrates the complexity of the neural network from a functional perspective.

4. Discussion

The triggered effects of synchronised HFS have been shown to be neurally mediated, and we have provided further evidence with phenomenon observed during synchronised HFS (Schauerte et al., 2001;

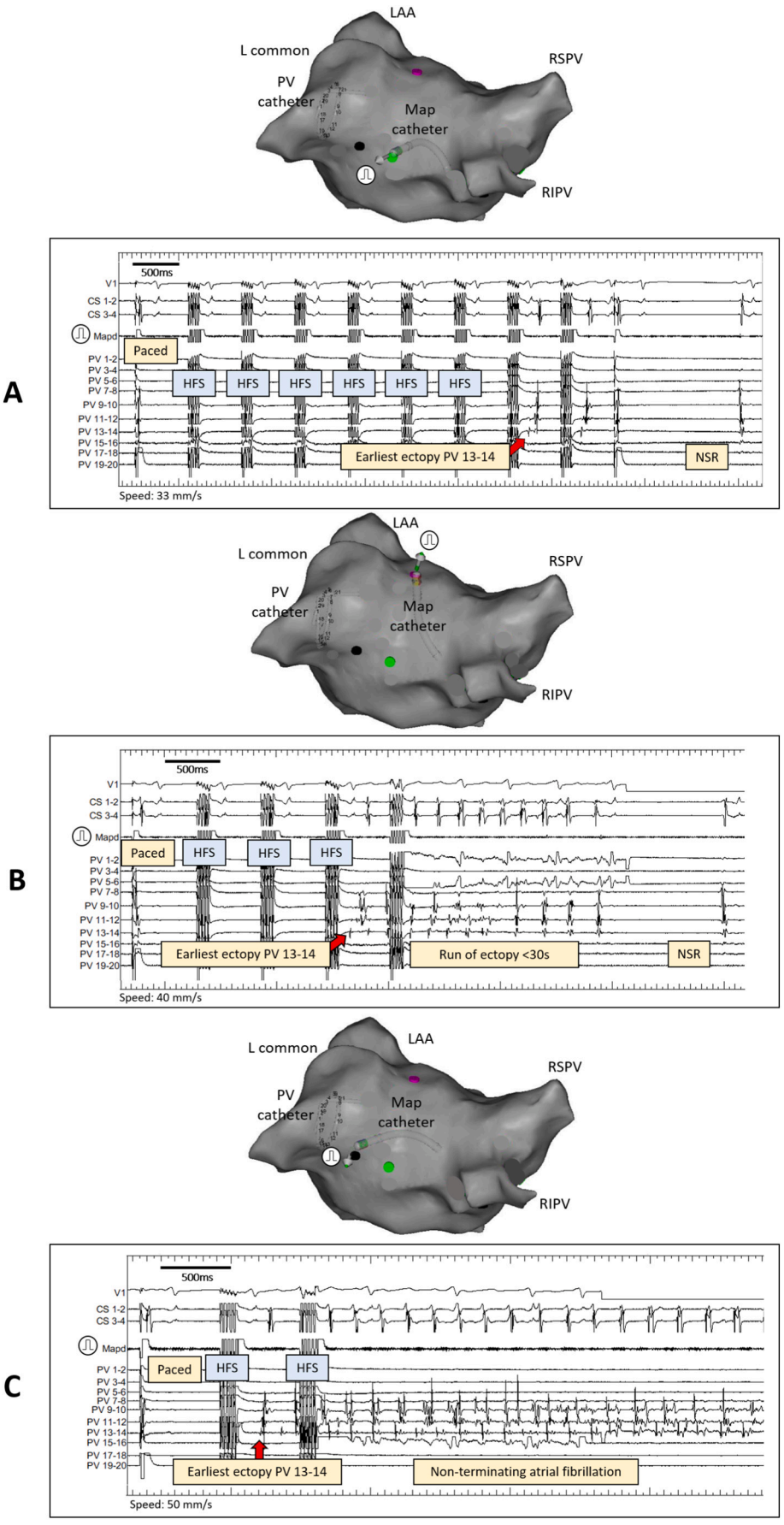

Fig. 2. Intracardiac electrograms of the range of responses to HFS at ET-GP. All examples are from one patient. Map distal was used to pace and deliver HFS. Its positions in the LA at the time of stimulation are shown in the PA views of the CARTO™ geometry. The PV catheter was in the lower branch of the left common PV for all three ET-GP sites.

A) The Map catheter was positioned in the mid-roof, near to the posterior wall of the LA. After the first paced beat, the subsequent trains were synchronised HFS. The earliest ectopy activation was in PV 13–14. There were just two beats of the same ectopy before stopping both HFS and pacing.

B) The Map catheter was positioned near the anterior ostium of the upper branch of the left common PV. After the first paced beat, the subsequent trains were synchronised HFS. Again, the earliest ectopy activation was seen in PV 13–14. The PV rapidly fired causing few seconds of AF that regularised towards the end then terminated.

C) The Map catheter was positioned at the posterior ostium of the lower branch of the left common PV. This trace shows the first paced beat followed by one synchronised HFS train which triggered ectopy. The earliest ectopy activation was again in PV 13–14. This initiated sustained AF lasting > 2min. The patient had direct DC cardioversion to restore sinus rhythm.

(L = left, CS = coronary sinus, ET-GP = ectopy-triggering ganglionated plexus, HFS = high frequency stimulation, LA = left atrial, LAA = left atrial appendage, Map = mapping catheter, PA = posterior anterior, RSPV = right superior pulmonary vein, RIPV = right inferior pulmonary vein, PV = pulmonary vein).

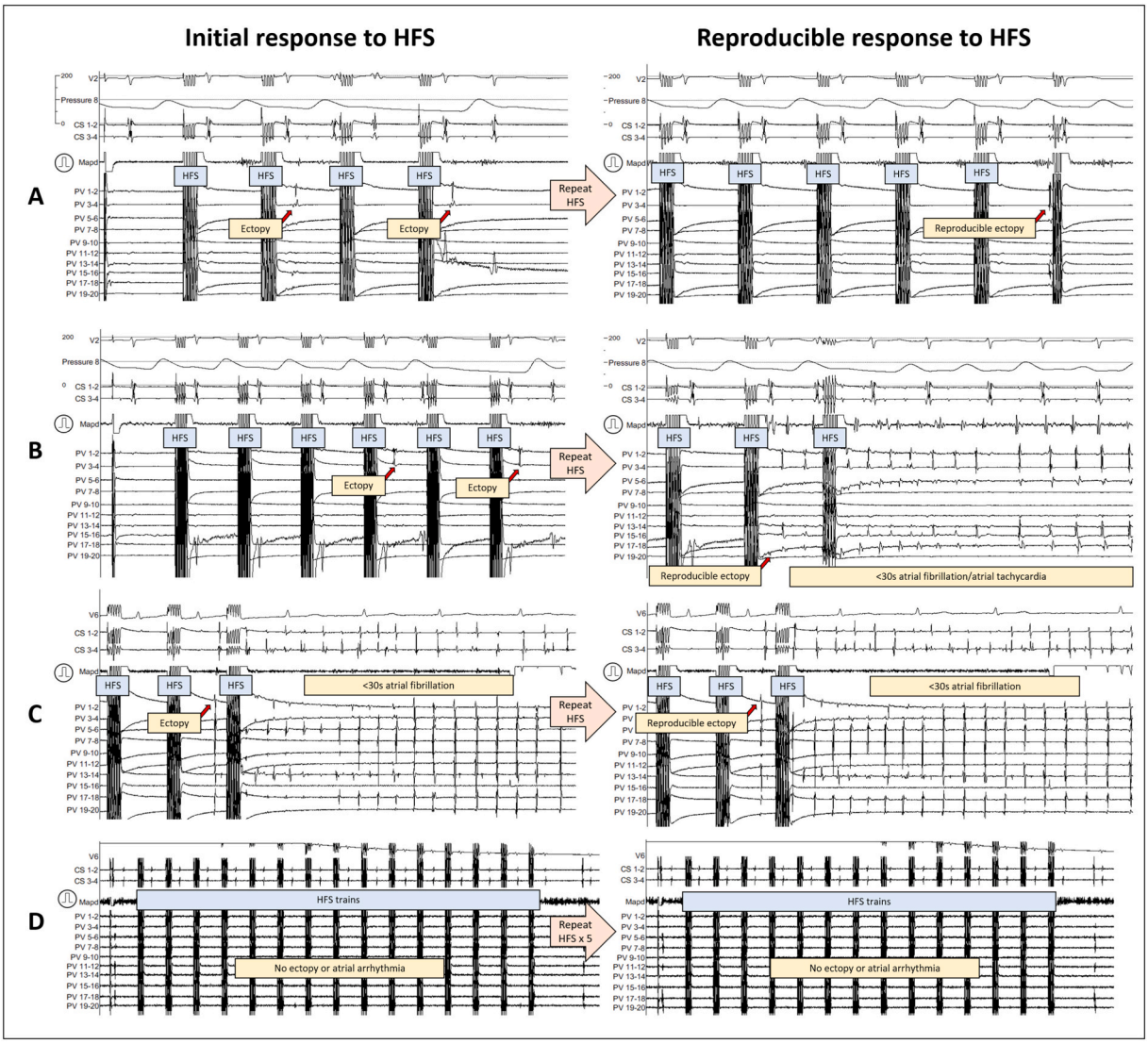

Fig. 3. Intracardiac recordings of ET-GP response reproducibility with synchronised HFS. A and B are from the same patient. C and D are from two different patients. In all the examples, pacing and HFS are delivered from the Map catheter.
A) In the left panel, a second train of HFS produced a PV ectopy which repeated itself after two further HFS. This response was reproducible upon re-testing the same site with HFS in the right panel. The PV ectopy in the right panel has different activation pattern to the left panel PV ectopy. The Map catheter was in the left side of the mid-posterior wall. The PV catheter was in the LIPV.
B) In the same patient as A), a different site was tested with HFS in the left panel. This produced a PV ectopy after the 4th train of HFS, which repeated after 2 further HFS trains. Upon re-testing the same site with HFS, the right panel shows an early PV ectopy in PV 17–18 which initiated rapid PV discharges, causing 3.5 s of AF. The Map catheter was near the base of the LIPV in the posterior wall, 10 mm superior to the Map position from A). The PV catheter was in the LIPV.
C) In a different patient to A/B), a PV ectopy initiated after several trains of HFS which induced 7.6 s of AF. Re-testing this site in the right panel showed repeated PV ectopy which induced 4.5 s of AF. The Map catheter was at the base and ostium of the LIPV in the posterior wall. The PV catheter was in the LIPV.
D) In a different patient to A/B) and C), one negative HFS site was re-tested five times, with no positive response to HFS in each re-test. The Map catheter was medial to the appendage in the anterior wall and the PV catheter was in the left superior PV. This was repeated in 9 other patients which produced the same outcome of negative responses to HFS with up to five re-tests at the same site.
(Same abbreviations as in Fig. 1)

Lim et al., 2011b; Scherlag et al., 2005). The distribution and characteristics of ET-GP in patients with AF help to explain some of the clinical phenomena described during and after PV isolation (PVI) for AF and support the development of a strategy for autonomic modulation.

4.1. The ganglionated plexuses

GP sites that cause AV-dissociation (AVD-GP) have been frequently cited in clinical studies for AF ablation, with the assumption that it is involved in the arrhythmogenesis of AF. However, PV ectopy is known to trigger AF and this was replicated with synchronised HFS within the local myocardial refractory period at ET-GP (Schauerte et al., 2001; Lim et al., 2011a). HFS within the local myocardial refractory period stimulate the intracardiac nerves without direct myocardial capture. Smaller nerves branch out from the epicardial GP and are located throughout transmural atrial tissue (Cho et al., 2019), and would also stimulate with HFS. A detailed study on the muscle connection and autonomic nerve distribution in the PV-LA junction of the LA showed that both adrenergic and cholinergic nerves were equally spatially distributed along the longitudinal and transmural axes of the PV-LA segments and circumferentially around the PV orifice (Tan et al., 2006). We are likely stimulating both types of nerves with HFS, and this may

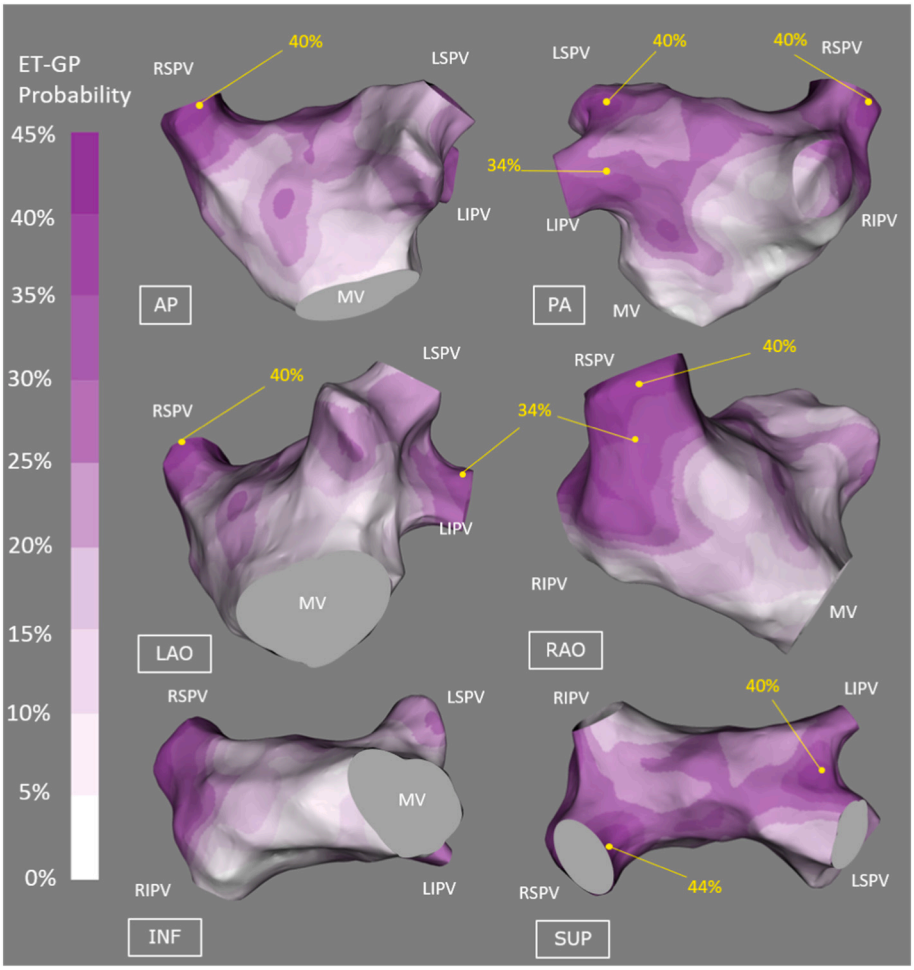

Fig. 4. The probability distribution atlas of ET-GPs. The probabilities are between 0 and 45%, white to dark purple. "High probability ET-GP sites" were defined as > 30% in probability, labelled with yellow dots on the atlas. This corresponds to the upper third probability (30–45%) of ET-GP. The highest probability of finding ET-GPs were in the roof and around the PV ostia. (For interpretation of the references to colour in this figure legend, the reader is referred to the web version of this article.)

be the neural composition of ET-GP as we found these to be mostly in the PV-LA junction. Neural stimulation lead to abundant acetylcholine and catecholamine release, which shortens the action potential of the local and adjacent myocardial cells, inducing atrial ectopy and arrhythmia (Patterson et al., 2005; Singh et al., 1999; Chen et al., 2014). The action potential normalises within two beats of HFS cessation (Schauerte et al., 2001).

4.2. The interconnecting neural network of GP

The GP are part of the intricately interconnected autonomic network. The "right lower GP" near the base of the right inferior PV act as an 'integration centre' for AV dissociating effects from other GP areas in the atria (Hou et al., 2007). Similarly, stimulation of the GP near the anterior portion of the right superior PV act as the integration centre for slowing of the heart rate and shortening the effective refractory period via the sinoatrial node (Ardell and Randall, 1986; Quan et al., 1999). Ablation at these integration centres abolish their stimulation effects at distant sites (Hou et al., 2007; Malcolme-Lawes et al., 2013).

The current study also demonstrated that ET-GP stimulated at one location in the LA can trigger electrical changes at another without any apparent effect on the myocardium in between the two locations. PVI can transect the neural communication between ET-GP and the isolated PV, and direct ablation over an ET-GP site abolishes its effects of triggering ectopy (Katritsis et al., 2008). The probability atlas from this study shows a preponderance of ET-GP in the PV antra and may explain why circumferential PV antral (CPVA) ablation is superior to segmental isolation, by transecting the GP neural connections into the PVs. This model may explain why 58.6% patients can have of at least one PV reconnected at follow-up mapping without recurrence of AF (Nery et al., 2016). These findings from the ET-GP distribution and behaviour may finally explain some of the inconsistencies from PV isolation simply being about preventing activation exiting the veins.

4.3. Functional and anatomical locations of ET-GP and AVD-GP

We densely mapped the whole LA with synchronised HFS to identify their distinct anatomical sites. The high probability (> 30%) sites of ET-GP was consistent with previous anatomical and clinical studies of GP (Haïssaguerre et al., 1998; Hsieh et al., 1999; Lau et al., 1999). Interestingly, there were discrete regions that were absent from ET-GP such as the right side of the posterior wall and the base of the right inferior PV. These regions are likely occupied by AVD-GP, as we described previously (Kim et al., 2018). Similarly, the regions that are absent of AVD-GP are likely occupied by ET-GP. These anatomical differences are important to distinguish to deliver the correct HFS technique to identify all GP.

4.4. Differences in GP responses to HFS

We demonstrated a range of responses with synchronised HFS at an ET-GP site. This may be related to the degree of GP stimulation which can be controlled by the amount of current delivered to the site (Schauerte et al., 2001; Scherlag et al., 2002), which in turn affects the actional potential and atrial effective refractory period shortening. Therefore, a single ectopy-triggering GP site with HFS may be capable of inducing AF with more prolonged HFS or increased current delivery to the GP site (Schauerte et al., 2001).

Occasionally, we observed a progressive Wenckebach with or without ectopy when testing a GP site with synchronised HFS, as previously reported by Lim et al., 2011. Re-testing the site with continuous HFS showed a more pronounced RR prolongation, reaching the threshold for an AVD-GP site. As synchronised HFS can identify both ET-GP and AVD-GP, we would have expected to see more AVD-GP in the posterior wall but found only a few. This may be due to not adequately reaching the threshold for stimulating AVD-GP with shorter bursts of HFS trains used with synchronised HFS.

4.5. Clinical implications

In clinical studies, continuous HFS has been commonly used to identify AVD-GP as targets for autonomic modulation in AF (Driessen et al., 2016; Katritsis et al., 2008). However, continuous HFS does not identify all GP. ET-GP and AVD-GP have very different anatomical and functional characteristics that need to be distinguished to target the relevant GP.

The current standard ablative treatment for AF is complete PVI via CPVA (Kirchhof et al., 2017). CPVA would invariably ablate many ET-GP that are located in the roof and around the PV ostia. This is in effect, both PVI and GP ablation procedure. However, the results from this study demonstrate that there are ET-GP outside the conventional CPVA lines. It is not known whether ET-GP ablation may confer additional benefit to CPVA alone in prevention of AF.

4.6. Limitations

The effect of general anaesthesia on patients' autonomic response to HFS is not known. Co-location of ET-GP and AVD-GP has been identified in some patients, but this has not been consistently tested across all patients as the focus of this paper was in the ET-GP distribution of the LA. Endocardial HFS may not reach to stimulate all GP in the epicardium, and therefore we may be underestimating the quantity of ET-GP in each patient in this study. The morphology of intracardiac electrograms at ET-GP sites were not analysed in this study. It was not possible to prove that synchronised HFS exclusively stimulates the intrinsic nerves or the GP in this clinical study. Further mechanistic studies are warranted to provide evidence for neural activation with synchronised HFS.

5. Conclusion

This study gives further insight into the variation and complexity of the intrinsic cardiac autonomic network in humans. ET-GP stimulation with synchronised HFS displays a wide range of responses from few beats of ectopy to sustained AF, and occasionally AV block with or without atrial arrhythmia. There are distinct high and low probabilities regions of ET-GP in patients with AF, and their anatomical distribution is markedly different to AVD-GP. ET-GP preponderance to the roof and the PV ostia suggest that they are inadvertently ablated during circumferential PVI, which is likely to alter GP function and may contribute to outcomes.

Supplementary data to this article can be found online at https://doi.org/10.1016/j.autneu.2020.102699.

Declaration of competing interest

None.

Acknowledgements

This study and some of the authors (BS, FSN, ZW NWFL) were part-funded by British Heart Foundation, UK; British Cardiac Trust, UK funded MYK; Rosetrees Trust, UK part-funded MYK, BHF Centre of Research Excellence, UK part-funded MYK and St Mary's Coronary Flow Trust, UK part-funded MYK. The department is supported by the National Institute for Health Research (NIHR) Biomedical Research Centre based at Imperial College Healthcare NHS Trust and Imperial College London. The views expressed are those of the author(s) and not necessarily those of the NHS, the NIHR or the Department of Health.

Funding

British Cardiac Trust; British Heart Foundation, Grant/Award Number: FS/13/73/30352; St Mary's Coronary Flow Trust, Rosetrees Trust, BHF Centre of Research Excellence.

References

Ali, R.L., Cantwell, C.D., Qureshi, N.A., Roney, C.H., Lim, P.B., Sherwin, S.J., Siggers, J.H., Peters, N.S., 2015. Automated fiducial point selection for reducing registration error in the co-localisation of left atrium electroanatomic and imaging data. In: Proc Annu Int Conf IEEE Eng Med Biol Soc EMBS, pp. 1989–1992 2015-Novem.

Ardell, J.L., Randall, W.C., 1986. Selective vagal innervation of sinoatrial and atrioventricular nodes in canine heart. Am. J. Physiol. Heart Circ. Physiol. 251, H764–H773.

Armour, J.A., Murphy, D.A., Yuan, B.X., Macdonald, S., Hopkins, D.A., 1997. Gross and microscopic anatomy of the human intrinsic cardiac nervous system. Anat. Rec. 247, 289–298.

Chen, P.S., Chen, L.S., Fishbein, M.C., Lin, S.F., Nattel, S., 2014. Role of the autonomic nervous system in atrial fibrillation: pathophysiology and therapy. Circ. Res. 114, 1500–1515.

Cho, K.H., Kim, J.H., Murakami, G., Abe, H., Rodríguez-Vázquez, J.F., Chai, O.H., 2019. Nerve distribution in myocardium including the atrial and ventricular septa in late stage human fetuses. Anat. Cell Biol. 52, 48–56.

Driessen, A.H.G., Berger, W.R., Krul, S.P.J., Berg, N.W.E. van den, Neefs, J., Piersma, F.R., Chan Pin Yin, D.R.P.P., Jong, J.S.S.G. de, Boven, W.P. van, Groot, J.R. de, 2016. Ganglion plexus ablation in advanced atrial fibrillation. J. Am. Coll. Cardiol. 68, 1155–1165.

Haïssaguerre, M., Jaïs, P., Shah, D.C., Takahashi, A., Hocini, M., Quiniou, G., Garrigue, S., Mouroux, A. Le, Métayer, P. Le, Clémenty, J., 1998. Spontaneous initiation of atrial fibrillation by ectopic beats originating in the pulmonary veins. N. Engl. J. Med. 339, 659–666.

Hou, Y., Scherlag, B.J., Lin, J., Zhou, J., Song, J., Zhang, Y., Patterson, E., Lazzara, R., Jackman, W.M., Po, S.S., 2007. Interactive atrial neural network: determining the connections between ganglionated plexi. Heart Rhythm 4, 56–63.

Hsieh, M.H., Chen, S.A., Tai, C.T., Tsai, C.F., Prakash, V.S., Yu, W.C., Liu, C.C., Ding, Y.A., Chang, M.S., 1999. Double multielectrode mapping catheters facilitate radiofrequency catheter ablation of focal atrial fibrillation originating from pulmonary veins. J. Cardiovasc. Electrophysiol. 10, 136–144.

Katritsis, D., Giazitzoglou, E., Sougiannis, D., Goumas, N., Paxinos, G., Camm, A.J., 2008. Anatomic approach for ganglionic plexi ablation in patients with paroxysmal atrial fibrillation. Am. J. Cardiol. 102, 330–334.

Kim, M.Y., Sikkel, M.B., Hunter, R.J., Haywood, G.A., Tomlinson, D.R., Tayebjee, M.H., Ali, R.L., Cantwell, C.D., Gonna, H., Sandler, B.C., Lim, E., Furniss, G., Panagopoulos, D., Begg, G., Dhillon, G., Hill, N.J., O'Neill, J., Francis, D.P., Lim, P.B., Peters, N.S., Linton, N.W.F., Kanagaratnam, P., 2018. A novel approach to mapping the atrial ganglionated plexus network by generating a distribution probability atlas. J. Cardiovasc. Electrophysiol. 29, 1624–1634.

Kirchhof, P., Benussi, S., Zamorano, J.L., Aboyans, V., Achenbach, S., Agewall, S., Badimon, L., Barón-Esquivias, G., Baumgartner, H., Bax, J.J., Bueno, H., Carerj, S., Dean, V., Erol, Ç., Fitzsimons, D., Gaemperli, O., Kirchhof, P., Kolh, P., Lancellotti, P., Lip, G.Y.H., Nihoyannopoulos, P., Piepoli, M.F., Ponikowski, P., Roffi, M., Torbicki, A., Carneiro, A.V., Windecker, S., Hayrapetyan, H.G., Roithinger, F.X., Aliyev, F., et al., 2017. 2016 ESC guidelines for the management of atrial fibrillation developed in collaboration with EACTS. Russ. J. Cardiol. 147, 7–86.

Lau, C.P., Tse, H.F., Ayers, G.M., 1999. Defibrillation-guided radiofrequency ablation of atrial fibrillation secondary to an atrial focus. J. Am. Coll. Cardiol. 33, 1217–1226 Elsevier Masson SAS.

Lim, P.B., Malcolme-Lawes, L.C., Stuber, T., Wright, I., Francis, D.P., Davies, D.W., Peters, N.S., Kanagaratnam, P., 2011a. Intrinsic cardiac autonomic stimulation induces pulmonary vein ectopy and triggers atrial fibrillation in humans. J. Cardiovasc. Electrophysiol. 22, 638–646.

Lim, P.B., Malcolme-Lawes, L.C., Stuber, T., Kojodjojo, P., Wright, I.J., Francis, D.P., Wyn

Davies, D., Peters, N.S., Kanagaratnam, P., 2011b. Stimulation of the intrinsic cardiac autonomic nervous system results in a gradient of fibrillatory cycle length shortening across the atria during atrial fibrillation in humans. J. Cardiovasc. Electrophysiol. 22, 1224–1231.

Malcolme-Lawes, L.C., Lim, P.B., Wright, I., Kojodjojo, P., Koa-Wing, M., Jamil-Copley, S., Dehbi, H.M., Francis, D.P., Davies, D.W., Peters, N.S., Kanagaratnam, P., 2013. Characterization of the left atrial neural network and its impact on autonomic modification procedures. Circ. Arrhythmia Electrophysiol. 6, 632–640.

Nery, P.B., Belliveau, D., Nair, G.M., Bernick, J., Redpath, C.J., Szczotka, A., Sadek, M.M., Green, M.S., Wells, G., Birnie, D.H., 2016. Relationship between pulmonary vein reconnection and atrial fibrillation recurrence: a systematic review and meta-analysis. JACC Clin. Electrophysiol. 2, 474–483.

Patterson, E., Po, S.S., Scherlag, B.J., Lazzara, R., 2005. Triggered firing in pulmonary veins initiated by in vitro autonomic nerve stimulation. Heart Rhythm 2, 624–631.

Pokushalov, E., Romanov, A., Shugayev, P., Artyomenko, S., Shirokova, N., Turov, A., Katritsis, D.G., 2009. Selective ganglionated plexi ablation for paroxysmal atrial fibrillation. Heart Rhythm 6, 1257–1264 Elsevier Inc.

Quan, K.J., Lee, J.H., Geha, A.S., Biblo, L.A., Van Hare, G.F., Mackall, J.A., Carlson, M.D., 1999. Characterization of sinoatrial parasympathetic innervation in humans. J. Cardiovasc. Electrophysiol. 10, 1060–1065.

Scanavacca, M., Pisani, C.F., Hachul, D., Lara, S., Hardy, C., Darrieux, F., Trombetta, I., Negrão, C.E., Sosa, E., 2006. Selective atrial vagal denervation guided by evoked vagal reflex to treat patients with paroxysmal atrial fibrillation. Circulation 114, 876–885.

Schauerte, P., Scherlag, B.J., Patterson, E., Scherlag, M.A., Matsudaria, K., Nakagawa, H., Lazzara, R., Jackman, W.M., 2001. Focal atrial fibrillation: experimental evidence for a pathophysiologic role of the autonomic nervous system. J. Cardiovasc. Electrophysiol. 12, 592–599.

Scherlag, B.J., Yamanashi, W.S., Schauerte, P., Scherlag, M., Sun, Y.X., Hou, Y., Jackman, W.M., Lazzara, R., 2002. Endovascular stimulation within the left pulmonary artery to induce slowing of heart rate and paroxysmal atrial fibrillation. Cardiovasc. Res. 54, 470–475.

Scherlag, B.J., Nakagawa, H., Jackman, W.M., Yamanashi, W.S., Patterson, E., Po, S., Lazzara, R., 2005. Electrical stimulation to identify neural elements on the heart: their role in atrial fibrillation. J. Interv. Card. Electrophysiol. 13 (Suppl. 1), 37–42.

Singh, S., Johnson, P.I., Javed, A., Gray, T.S., Lonchyna, V.A., Wurster, R.D., 1999. Monoamine- and histamine-synthesizing enzymes and neurotransmitters within neurons of adult human cardiac ganglia. Circulation 99, 411–419.

Tan, A.Y., Li, H., Wachsmann-Hogiu, S., Chen, L.S., Chen, P.S., Fishbein, M.C., 2006. Autonomic innervation and segmental muscular disconnections at the human pulmonary vein-atrial junction. Implications for catheter ablation of atrial-pulmonary vein junction. J. Am. Coll. Cardiol. 48, 132–143.